

RESEARCH

Open Access



Meprin β regulates osteopontin-signaling in ischemia/reperfusion-induced kidney injury

Faihaa Ahmed^{1,2}, Shaymaa Abousaad¹, Ayman Abouzeid³, Christine Adhiambo¹ and Elimelda Moige Onger^{1*}

Abstract

Background Meprin metalloproteases have been implicated in the pathology of ischemia/reperfusion (IR) induced kidney injury. Meprin β proteolytically processes several mediators of cell signaling pathways involved in apoptosis and extracellular matrix metabolism. We previously showed that meprin β cleaves osteopontin (OPN) *in vitro*. The objective of the current study was to determine how meprin β expression affects OPN and downstream mediators of the OPN-signaling pathway in IR-induced kidney injury.

Methods Ischemia/Reperfusion injury was induced in wild-type (WT) and meprin β knockout (β KO) mice. Blood samples and kidney tissues were obtained at 24 h post-IR. The levels of OPN, Caspase-3, Bcl-2, and NF κ B were evaluated using real-time PCR, western blot, and immunohistochemical approaches. Data analysis utilized a combination of 2-way ANOVA and unpaired *t* test.

Results OPN mRNA increased in both genotypes at 24 h post-IR. Immunohistochemical staining showed IR-associated increases in the levels of OPN in both genotypes. Additionally, we observed higher levels of OPN in the lumen of proximal tubules in WT only, suggesting that meprin β contributes to enhanced release of OPN into filtrate and ultimately into urine. Immunohistochemical staining showed significant increases in the levels of Caspase-3 and NF κ B in select tubules of WT only, while Bcl-2 staining intensity increased significantly in both genotypes at 24 h post-IR.

Conclusions These findings suggest that meprin β modulates OPN levels in IR-induced kidney injury and impacts apoptotic genes regulated by the OPN signaling pathway.

Clinical trial number Not applicable.

Keywords Ischemia/reperfusion, Meprin, Osteopontin, Apoptosis

*Correspondence:

Elimelda Moige Onger
eonger@ncat.edu

¹Department of Kinesiology, North Carolina A&T State University, Greensboro, NC 27411, USA

²Department of Biology, North Carolina A&T State University, Greensboro, NC 27411, USA

³Department of Agribusiness, Applied Economics and Agriscience Education, North Carolina A&T State University, Greensboro, NC 27411, USA



© The Author(s) 2025. **Open Access** This article is licensed under a Creative Commons Attribution-NonCommercial-NoDerivatives 4.0 International License, which permits any non-commercial use, sharing, distribution and reproduction in any medium or format, as long as you give appropriate credit to the original author(s) and the source, provide a link to the Creative Commons licence, and indicate if you modified the licensed material. You do not have permission under this licence to share adapted material derived from this article or parts of it. The images or other third party material in this article are included in the article's Creative Commons licence, unless indicated otherwise in a credit line to the material. If material is not included in the article's Creative Commons licence and your intended use is not permitted by statutory regulation or exceeds the permitted use, you will need to obtain permission directly from the copyright holder. To view a copy of this licence, visit <http://creativecommons.org/licenses/by-nc-nd/4.0/>.

Introduction

Meprins metalloproteinases are abundantly expressed in the brush-border membranes (BBM) of kidney proximal tubules and small intestines. Meprins are also expressed in leukocytes (monocytes and macrophages) [1] and in podocytes under certain pathological conditions. Meprin have been implicated in the pathophysiology of acute kidney injury (AKI) induced by ischemia-reperfusion (IR) [2, 3] and chronic kidney injury induced by diabetes [4, 5]. During IR-induced acute kidney injury, meprins are redistributed from the BBM to the cytosol and basolateral compartments of proximal kidney tubules [2], bringing them into contact with proteins in these cell compartments with a role in modulating inflammation, apoptosis, cell survival and leukocytes infiltration [6]. However, the cellular and molecular mechanisms underlying meprin modulation of renal injury are not fully understood.

Meprins consist of two subunits, α and β , which combine to form two protein isoforms: meprin A (α - α or α - β) and meprin B (β - β). Meprin B has been shown to proteolytically process osteopontin (OPN) in vitro [7]. However, it's not known if meprin β -OPN interactions impact the progression of kidney injury in vivo. OPN, a highly phosphorylated multifunctional glycoposphoprotein is produced by renal tubular epithelial cells, and expression is upregulated in glomerulonephritis, hypertension, IR-induced AKI, renal ablation, and unilateral ureteral obstruction [8], interstitial inflammation, and fibrosis [9]. In mice, OPN blockade attenuates renal injury after IR by inhibiting natural killer (NK) cell infiltration [10]. OPN mediates cell survival [11] and attenuates cell apoptosis [12, 13]. OPN was shown to regulate renal apoptosis and interstitial fibrosis in a unilateral ureteral obstruction chronic renal injury model [14]. Meprin β -OPN interaction could thus regulate kidney injury through interactions with various molecules involved in the injury response.

The objective of the current study was to determine how meprin β expression impacts downstream mediators of the OPN signaling pathway in the kidneys of mice subjected to IR-induced injury and gain insights on how proteolytic processing of OPN by meprin β modulates the mechanisms underlying-induced kidney injury.

Materials and methods

Experimental animals

Two genotypes were used; (1) wild-type (WT) mice which express normal levels of both meprin A and meprin B, and (2) meprin β knockout (β KO) mice in which the meprin β gene was disrupted. The β KO mice are deficient in meprin B (β - β) and the heterodimeric form of meprin A (α - β). The WT mice were purchased from Charles River Laboratories (Wilmington, MA).

Meprin β KO mice were initially obtained from the laboratory of Dr. Judith Bond (Pennsylvania State University) and bred in the Laboratory Animal Resource Unit (LARU) of North Carolina A&T State University (NC A&T). The randomly selected mice were housed in standard cages of up to 5 mice per cage in a 12 h light:12 h dark cycle and provided rodent chow and water *ad libitum*.

Ischemia/Reperfusion induced kidney injury

Twelve-week-old male mice (6 WT and 5 β KO) on a C57BL/6 background were subjected to nephrectomy and IR-induced injury using surgical procedures as previously described [4]. In summary, the mice weighing between 25 and 35 g were anesthetized intraperitoneally with a combination of Ketamine and Xylazine at 4.3 μ l/g body weight [15, 16]. Bilateral flank incisions and renal pedicle dissections were performed. Nephrectomy was used to excise the left kidney. The renal pedicle of the right kidney was clamped with a microvascular clamp (Roboz, Rockville, MD) for 27 min, maintaining a constant temperature and ensuring proper hydration throughout the procedure. After the ischemia period, the clamps were removed, and the incisions were sutured. Mice were injected with 0.05 ml/g body weight pre-warmed (37 °C) saline subcutaneously previously described [2, 4]. Then, the mice were placed in temperature-controlled cages for recovery. To manage pain, mice received Buprenorphine (3.5 μ l/g body weight) between 8 and 12 h post-surgery. At 24 h post-IR, the mice were then euthanized by CO₂ asphyxiations and kidney tissues harvested for gene and protein expression analysis. Nephrectomized kidneys collected at 0 h served as controls for each mouse.

Kidney injury assessment

Blood samples were obtained by tail nicking at 0 h and by cardiac puncture at 24 h post-IR. The blood samples were processed as previously described [4] to obtain plasma, which were stored in aliquots at -80 °C until used to assess kidney injury. Plasma levels of neutrophil gelatinase-associated lipocalin (NGAL) were assayed to confirm kidney injury using Enzyme-linked immunosorbent assays (ELISA). Previous studies by our group and others have established that serum creatinine (SCr) is less sensitive as a biomarker of acute kidney injury (AKI) when compared to NGAL and Cystatin C, especially in the early phase [17–24]. The ELISA utilized commercial NGAL assay kits (R&D Systems, Minneapolis, MN) and followed the manufacturer's instructions. A Tecan Infinite 200 PRO plate reader (Tecan, Untersbergstraße, Austria) was used to read absorbance at nm 540 and nm 450. GraphPad Prism 7.0 software was used for generating standard curves, extrapolating values for the ELISA assays, and for subsequent statistical analysis of the data.

Processing kidney tissue

The excised kidneys were decapsulated and sectioned into three parts; (1) a 2 mm mid-section was processed for immunohistochemical analysis. This section was fixed in formaldehyde overnight at 4 °C then placed in 70% ethanol at 4 °C, before paraffin embedding, and sectioned onto slides. (2) a second section for protein extraction, was wrapped in aluminum foil, snap-frozen in liquid nitrogen, and stored at -80 °C. (3) a third section was processed for RNA extraction – this was placed in RNeasy Lysis Buffer (Qiagen, Waltham, MA) at 4 °C overnight. The RNeasy Lysis Buffer was then aspirated and the tissues stored at -80 °C.

RNA extraction and cDNA synthesis

The frozen kidney tissues were thawed on ice, homogenized using a tissue homogenizer (Bead Mill 4 Homogenizer, 2016 Thermo Fisher Scientific Inc). Total RNA was extracted using Qiagen's RNeasy Mini Kit, according to the manufacturer's protocol. Total RNA concentration and purity (260/280 and 260/230) were measured on a NanoDrop spectrophotometer 2000 (Thermo Scientific, Wilmington, DE). cDNA was synthesized by reverse-transcriptase using High-Capacity cDNA Reverse Transcription Kit with RNase inhibitors (ThermoFisher Scientific, Waltham, MA). The reverse transcription process was completed at 37 °C for 90 min, 85 °C for 3 min, quick chilling at 4 °C and synthesized cDNA was diluted and stored in -80 °C.

Real time PCR

We used OPN primers previously described [25]; forward 5'-AGCCACAAGTTTCACAGCCACAAGG-3', reverse 5'-CTGAGAAATGAGCAGTTAGTATTC TGC-3'. Primers for Caspase-3, Bcl-2 and NFκB were designed using gene sequences in the www.ncbi.nlm.nih.gov database and synthesized by ITDNA (Coralville, IA). Caspase-3 forward 5'-GAGCTTGAACGGTACGCTA-3', reverse 5'-CCGTACCAGAGCGAGATGAC-3'; Bcl-2: forward 5'-GCCTTTTCTCCTTTGGCGG-3', reverse 5'-AAGAGTGAGCCCAGCAGAAC-3'; NFκB forward 5'-ATT TGC AAC TAT GTG GGG CCT-3', reverse 5'-CTGTCATCCGTGCTTCCAGT-3'; GAPDH forward 5'-GGTGAAGGTCGGTGTGAACG-3', reverse 5'-CTCGCTCCTGGAAGATGGTG-3'. Two-steps Real Time PCR was performed using standardized quantities of cDNA using SYBR Green QPCR Master Mix kit. Amplified cDNA was generated and detected using Bio-Rad Multiplate™ 96-Well PCR Plates. Each PCR amplification condition was set up as follows: the first step was 50 °C for 2 min, 95 °C for 10 min followed by 40 cycles of a two-step amplification program (95 °C for 15 s and 58 °C for 1 min). Melting curve analysis was applied at the end of the amplification using the dissociation protocol

from the Sequence Detection System to exclude contamination with non-specific PCR products. Data were analyzed via $2^{-\Delta\Delta C_t}$ method [26] and mRNA expressions of target genes were presented as fold change (FC) relative to the WT control samples after normalization against the geometric mean of mRNA expression of the house-keeping gene GAPDH of triplicate combinations from 4 mice per group.

Protein extraction from kidney tissues

Protein extraction utilized previously described protocols [6, 24, 27]. In summary, kidney tissues were thawed on ice and homogenized in 9 volumes of homogenization buffer (0.02 mM HEPES pH 7.9, 0.015 mM NaCl, 0.1 mM Triton-X 100, 0.01 mM SDS, 1 mM Na₃VO₄) with protease and phosphatase inhibitors. RIPA buffer was used to obtain protein lysates from sections of the kidney tissue. Protein concentrations were determined by the Bradford protein assay method, using Bio-Rad's protein assay reagent (Bio-Rad, Hercules, CA) and stored in aliquots at -80 °C until analyzed by Western blot.

Western blot analysis

Protein levels of OPN, Caspase-3, Bcl-2 and NFκB, from kidney lysates were evaluated using western blot analysis (3 mice per treatment group). Proteins were separated by molecular weight on 12% Sodium Dodecyl Sulfate Polyacrylamide (SDS-PAGE) gels using previously described protocols [6, 24, 27]. Proteins were then transferred to nitrocellulose membranes, incubated with 5% FBS to block non-specific binding sites, and probed with specific antibodies. Antibodies used were rabbit polyclonal anti-OPN (Abcam Cat# ab8448, RRID: AB_306566) diluted 1:1000, rabbit monoclonal anti-Caspase-3 (Cell Signaling Technology Cat# 9662, RRID: AB_331439) diluted 1:1000, mouse monoclonal anti-Bcl-2 (Cell Signaling Technology Cat# 15071, RRID: AB_2744528) diluted 1:1000, and rabbit monoclonal anti-NFκB (Cell Signaling Technology Cat# 8242, RRID: AB_10859369) diluted 1:1000. Anti-β tubulin antibodies (Origene Cat# TA301569) diluted 1:5000 was used to detect tubulin as a loading control. Following the primary antibody incubations, the membranes were washed three times, for 10 min each in TBS-T. Secondary antibodies, either mouse or rabbit IgG (Bio-Rad, Hercules, CA) diluted 1:10,000 in TBS-T, were added onto the membranes and incubated for 1 h at room temperature or overnight at 4 °C. The membranes were then washed three times for 15 min each in TBS-T. To detect protein bands, the membranes were exposed to chemiluminescence substrates (Thermo Fisher Scientific, Waltham, MA) and exposed to X-Ray film. The X-ray film blots were scanned on an HP Scanjet 8300. Background staining was removed using Image J and the protein bands intensities were determined by densitometry using

Image Studio™ Lite Software. The optic densities (OD) for each protein band were normalized to the OD of the housekeeping β -tubulin bands to obtain the relative OD.

Immunohistological staining and microscopic analysis of kidney tissue

Tissue for immunohistochemical analysis were paraffin-embedded at the Wake Forest University Pathology Laboratories. For immunohistochemical staining, we used previously described protocols [6, 23]. Briefly, slide sections of kidney tissue were deparaffinized using xylene, 100% ethanol, 95% ethanol, and water. Antigen unmasking was done by boiling at 95 °C in 10 mM sodium citrate buffer, pH 6.0, for 10 min. To block nonspecific binding sites, the sections were incubated in 5% normal goat serum with 0.3% Triton-X-100 at room temperature for 1 h in a humidified chamber. Primary antibodies were diluted in PBS buffer with 1% BSA and 0.3% Triton-X-100 (PBS-T). The primary antibodies were applied to sections and incubated overnight at 4 °C or at room temperature for 1 h. Rabbit polyclonal anti-OPN (Abcam Cat# ab8448, RRID: AB_306566) diluted 1:200, rabbit monoclonal anti-Caspase-3 (Cell Signaling Technology Cat# 9662, RRID: AB_331439) diluted 1:500, mouse monoclonal anti-Bcl-2 (Cell Signaling Technology Cat# 15071, RRID: AB_2744528) diluted 1:400, and rabbit monoclonal anti- NF κ B (Cell Signaling Technology Cat# 8242, RRID: AB_10859369) diluted 1:400.

For standard immunostaining, we used the Vectastain® Elite® ABC Universal Kit Protocol (Vector Laboratories, Burlingame CA) following the manufacturer's instructions, with peroxidase substrate solution (DAB) (Vector Laboratories Cat# SK-4100, RRID: AB_2336382) applied to obtain brown staining. The sections were counterstained with hematoxylin (to stain the nuclei), washed and mounted with coverslips and left at room temperature overnight to dry.

The staining intensity of the tissue sections for the various proteins (OPN, Caspase-3, Bcl-2, and NF κ B) were evaluated using BZ-X700 Series all-in-one fluorescence (KEYENCE Corporation of America, Elmwood, NJ) and imaged using BZ-X700 analysis Software. Optical density (OD) was determined in ten (10) non-overlapping fields for tubular and ten non-overlapping fields for renal corpuscles at 60 X magnification from each section. The fields from the sections were obtained in a blinded manner and quantified using 8-bit images for calibrated OD values and OD standard using Image J analysis Software (ImageJ/Fiji 1.46).

Immunofluorescence staining

To determine localization of the proteins of interest, we used immunofluorescence counterstaining according to the previously described protocols [6, 21] with

two proximal tubule markers, meprin β in WT kidney sections (Goat Anti Mouse Meprin β Subunit/MEP1B Antigen Affinity purified Polyclonal Antibody (R and D Systems, Cat # AF3300, RRID: AB_2143451) diluted 1:100 and villin in β KO kidney sections (mouse monoclonal anti-villin antibodies, Santa Cruz Biotechnology Cat# sc-58897, RRID: AB_2304475) diluted 1:200 for 1 h at room temperature. The slides sections were then rinsed three times in PBS for 10 min each and incubated in fluorophore-conjugated secondary antibodies: chicken polyclonal anti-goat, Alexa Fluor 488 (Invitrogen, Cat# A-21467, RRID: AB_141893) for meprin β ; either chicken monoclonal anti-mouse, Alexa Fluor® 488 (Invitrogen Cat# A-21200, RRID: AB_2535786) or chicken polyclonal anti-rabbit, Alexa Fluor® 488 (Invitrogen, Cat# A21441, RRID: AB_2535859) for Villin; donkey monoclonal anti-rabbit, Alexa Fluor® 647 (Abcam Cat# ab150075, RRID: AB_2752244) for OPN, Caspase-3 and NF κ B; donkey polyclonal anti-mouse, Alexa Fluor® 647 (Abcam Cat# ab150107, RRID: AB_2890037) for Bcl-2. For reasons of antibody compatibility, the Bcl-2 immunostaining counterstained with rabbit polyclonal anti-villin (Abcam Cat# ab52102, RRID: AB_883445) in WT kidney sections diluted 1:50. 4,6-Diamidino-2-phenylindole (DAPI) (Vector Laboratories Cat# SK-4100, RRID: AB_2336382) was used for nuclei staining. Prolong anti-fade reagent (Life Technologies, Carlsbad CA) was applied before mounting the sections with coverslips. The tissue sections were evaluated for meprins, OPN, Caspase-3, Bcl-2, and NF κ B expression and localization using BZ-X700 Series all-in-one fluorescence microscope (KEYENCE Corporation of America, Elmwood, NJ) and imaged using BZ-X700 analysis Software. Immunofluorescence data was qualitative and intended to distinguish proximal tubules from distal tubules.

Statistical analysis

Two-way ANOVA was utilized for data analysis using (GraphPad 7.0 Prism Software, GraphPad, La Jolla, CA). Data for western blots utilized the relative optical densities (OD), relative the OD of the loading control, while data for immunohistochemical staining utilized the calibrated ODs. For mRNA expression data analysis, unpaired *t* test was utilized to perform genes expression analysis for each group with WT control serving as the baseline control. The data are presented as mean \pm SEM of 3–4 mice per group. An equal number of animals were used across all groups. A statistician performed statistical analysis in a blind manner to ensure that the findings are objective and unbiased. The *p* values \leq 0.05 were considered statistically significant.

Results

Kidney injury was demonstrated by plasma NGAL levels, with significant increases at 24 h post-IR in both WT ($P \leq 0.01$) and meprin β knockout mice ($P \leq 0.01$). However, the fold change was greater in WT mice when compared to β KO mice (14.7 vs. 2.3 fold increase) (Fig. 1A), confirming that meprin β expression associates with enhanced kidney injury as previously reported [6, 24].

Meprin β expression was associated with increased expressions and shedding of osteopontin into proximal kidney tubules

A previous in vitro study demonstrated that meprin β is capable of proteolytically processing OPN [7]. To determine the impact of meprin β expression on OPN levels in vivo, mRNA and protein expression of OPN were evaluated. Real-time PCR data showed that the mRNA levels for OPN increased significantly in both WT ($P \leq 0.01$) and β KO ($P \leq 0.05$) mice at 24 h post-IR (Fig. 1B). Western blot analysis detected a full length OPN protein band at 66 kDa, with significant increases ($P \leq 0.05$) in protein levels in WT at 24 h post-IR when compared to levels in control kidneys. This increase in OPN protein levels was not observed in the kidneys of β KO mice subjected to IR (Fig. 1C). Additionally, we detected a cleaved OPN fragment at 32 kDa, for which there were no significant changes in either genotype at 24 h IR post-IR (Fig. 1C). We used immunohistochemical staining and light microscopy to assess the localization of OPN in kidney sections and quantified the staining intensity using Image J. Our data showed a significant increase in the staining intensity of OPN in select tubules from WT ($P \leq 0.0001$) and a modest increase in β KO ($P \leq 0.05$) tubules at 24 h post-IR (Fig. 1D). Interestingly, the staining intensity for OPN in renal corpuscles significantly increased in both WT ($P \leq 0.001$) and β KO ($P \leq 0.001$) at 24 h post-IR (Fig. 1E). To determine whether meprin expression correlates with OPN expression in mice kidney sections, we used fluorescent counterstaining with proximal tubule (PT) markers (meprin β for WT and villin for β KO respectively). Our data show that the increase in OPN occurred in both proximal (PTs) and distal tubules (DTs) (Fig. 1F). However, higher levels of OPN were detected in the lumen of PTs from WT but not β KO kidneys, suggesting that meprin β is partly responsible for enhanced shedding and release of OPN into renal filtrate and ultimately into urine as previously reported [28–30]. Taken together, the data suggests that IR-induces increased expression of OPN in proximal tubules. However, in meprin expressing tubules, the OPN is proteolytically processed and shed into the lumen to be excreted in urine.

Meprin β expression correlates with expression of anti- and pro-apoptotic genes

OPN signaling has been shown to modulate apoptosis [13]. We therefore assessed the levels of the apoptosis regulator genes cysteine-aspartic acid protease 3 (Caspase-3), B-cell lymphoma/leukemia 2 (Bcl-2), and nuclear factor kappa B (NF κ B). The real-time PCR data demonstrated decreased Caspase-3 mRNA levels in WT ($P \leq 0.01$) and increased expression in β KO mice at 24 h post-IR (Fig. 2A). Western blot analysis showed increases in caspase-3 protein levels; two bands (33 and 35 kDa) were detected with significant increase ($P \leq 0.0001$) in 33 kDa band in WT kidneys only (Fig. 2B). Increases in Caspase-3 protein levels were confirmed using light microscopy, with immunostaining intensity for Caspase-3 being significantly higher in select tubules of WT at 24 h post-IR ($P \leq 0.0001$) (Fig. 2C). In contrast, there was no significant change in Caspase-3 levels in β KO kidney tubules or interstitial tissues at 24 h post-IR (Fig. 2C). Protein staining intensity of renal corpuscles increased significantly in both WT ($P \leq 0.0001$) and β KO ($P \leq 0.0001$) at 24 h post-IR (Fig. 2D). Counterstaining of Caspase-3 with meprin β showed that the increased expression of Caspase-3 is in both proximal and distal tubules of WT at 24 h post-IR. In contrast, the β KO mice showed comparable expression levels of Caspase-3 (Fig. 2E). This increase in Caspase-3 expression in kidney tubules of WT, may in part correlate to meprin β expression and thus enhances tubular cell death and collectively the level of IR injury.

We used a similar approach to evaluate the expression of the anti-apoptotic and cell survival gene Bcl-2. Real-time PCR analysis showed no significant change in Bcl-2 mRNA levels in WT but significant increases in β KO kidneys ($P \leq 0.05$) at 24 h post-IR, (Fig. 3A). Interestingly, western blot analysis showed opposite patterns with a significant increase ($P \leq 0.05$) in Bcl-2 protein levels in WT kidneys at 24 h post-IR, but not in β KO mice (Fig. 3B). Immunohistochemical staining coupled with light microscopy analysis showed that the increase in protein level for Bcl-2 in WT kidney tubules was not global, but only in select tubules ($P \leq 0.0001$). For β KO kidneys, the levels were significantly higher ($P \leq 0.01$) in select kidney tubules as well as interstitial cells (presumed to be macrophages/dendritic cells) (Fig. 3C). Staining intensity for Bcl-2 in renal corpuscle tissue increased significantly in both WT ($P \leq 0.05$) and β KO ($P \leq 0.0001$) (Fig. 3D). To assess the localization of synthesized Bcl-2 in kidney tubules, we used immunofluorescence, counterstaining with villin a proximal tubule marker in both genotypes [27]. Our data showed that Bcl-2 expression levels increased in both proximal and distal renal tubules for WT kidneys. In β KO kidneys, Bcl-2 levels increased in both renal tubules and interstitial tissues (Fig. 3C). The

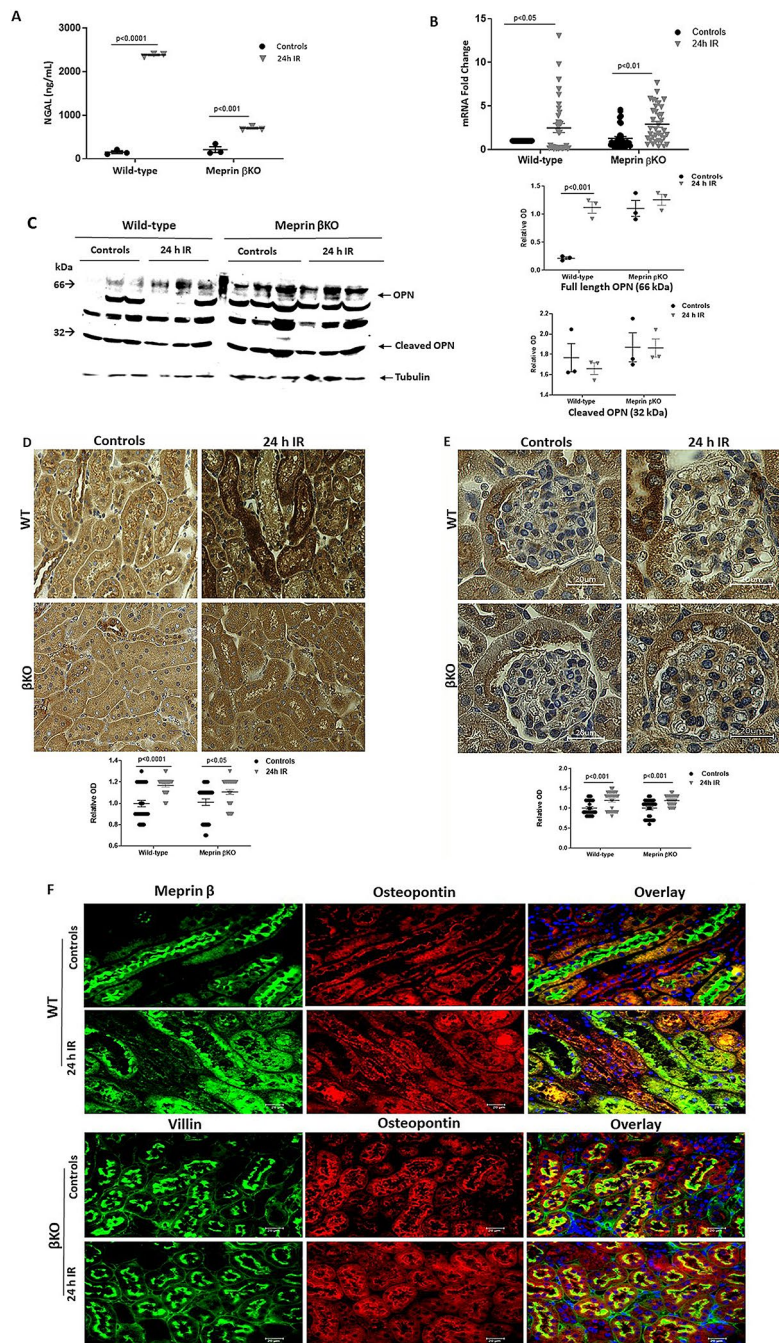


Fig. 1 Kidney injury biomarkers and OPN expression in kidney tissue from wild type (WT) and meprin β deficient mice (β KO) at 0 h (control) and 24 h post-IR. Kidney injury was confirmed using ELISA to assess the level of kidney injury biomarker, NGAL which significantly increased in both genotypes at 24 h post-IR (**A**). Blood samples were collected at 0 h and 24 h post-IR injury to assess the plasma levels of NGAL in 4 mice/group. Real-time-PCR analysis showed significant increases in OPN mRNA levels in both genotypes at 24 h post-IR (**B**). OPN mRNA levels are expressed as fold change (FC) relative to the WT control and normalized to GAPDH mRNA and each value represents the mean \pm SEM of triplicate combinations from 4 mice per group. Western blot analysis for OPN in kidney proteins from WT and meprin β KO mice showed IR-associated increased levels of the full-length OPN (66 KDa) in WT only (**C**). The protein bands represent samples from individual kidneys ($n = 3$). The relative optic densities (ODs) were calculated by normalizing the ODs of OPN to the ODs for β -tubulin in the same sample. The full-length images of western blot are presented in supplementary figure (S1). Immunohistochemical staining for OPN showed significant increase in WT and meprin β KO kidney tubules (**D**) and renal corpuscles of WT and meprin β KO (**E**). OD data were quantified ($n = 3$) using Image J analysis Software (ImageJ/Fiji 1.46) and analyzed for 10 non-overlapping fields from tubular and renal corpuscle sections from each kidney. Images at 60 \times magnification and the scale bar representing 20 μ m. Immunofluorescence counterstaining of OPN (red) with either meprin β (green) in WT mice or villin (PT marker, green) in meprin β -deficient mice showed that meprin β induced expression of OPN in PTs in kidneys subjected to IR (**F**). DAPI was used to stain the nuclei (blue). Images at 60 \times magnification and the scale bar representing 20 μ m. Data is expressed as mean \pm SEM with P values as indicated, $P \leq 0.05$ are considered statistically significant

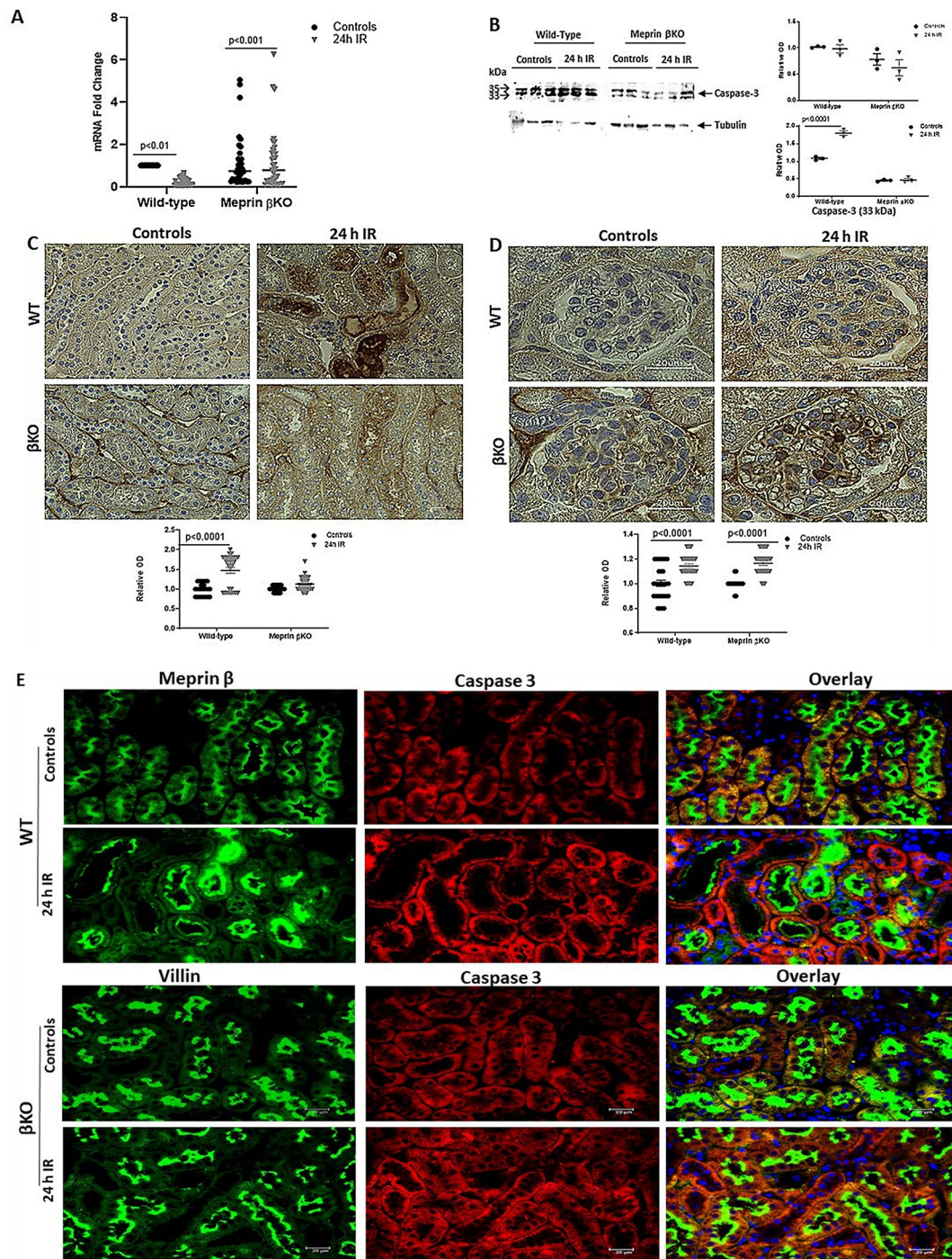


Fig. 2 Caspase-3 expression in kidney tissue from WT and meprin β KO mice at 0 h and 24 h post-IR. The real-time PCR data showed that mRNA expression levels of Caspase-3 decreased in WT and increased in β KO mice at 24 h post-IR (**A**). Caspase-3 mRNA levels are expressed as fold change (FC) relative to the WT control and normalized to GAPDH mRNA and each value represents the mean \pm SEM of triplicate combinations from 4 mice per group. Western blot analysis detected two bands of Caspase-3 (33 and 35 kDa) with significant increase in the Caspase-3 (33 kDa) band for WT kidneys only (**B**). The protein bands represent samples from individual kidneys ($n = 3$). The relative optic densities (ODs) were calculated by normalizing the ODs of Caspase-3 to the ODs for β -tubulin in the same sample. The full-length images of western blot are presented in supplementary figure (S2). Immunohistochemical staining of Caspase-3 showed significant increase in select tubules from WT kidney only (**C**) and renal corpuscles of both genotypes (**D**). OD data were quantified ($n = 3$) using Image J analysis Software (ImageJ/Fiji 1.46) and analyzed for 10 non-overlapping fields from tubular and renal corpuscle sections. Images at 60 \times magnification and the scale bar representing 20 μ m. Immunofluorescence counterstaining of Caspase-3 (red) with either meprin β (green) in WT or villin (PT marker, green) in meprin β -deficient mice showed that Caspase-3 increased in both PTs and DTs of WT but not in meprin β KO mice (**E**). DAPI was used to stain the nuclei (blue). Images at 60 \times magnification and the scale bar representing 20 μ m. Data is expressed as mean \pm SEM with P values as indicated, $P \leq 0.05$ are considered statistically significant

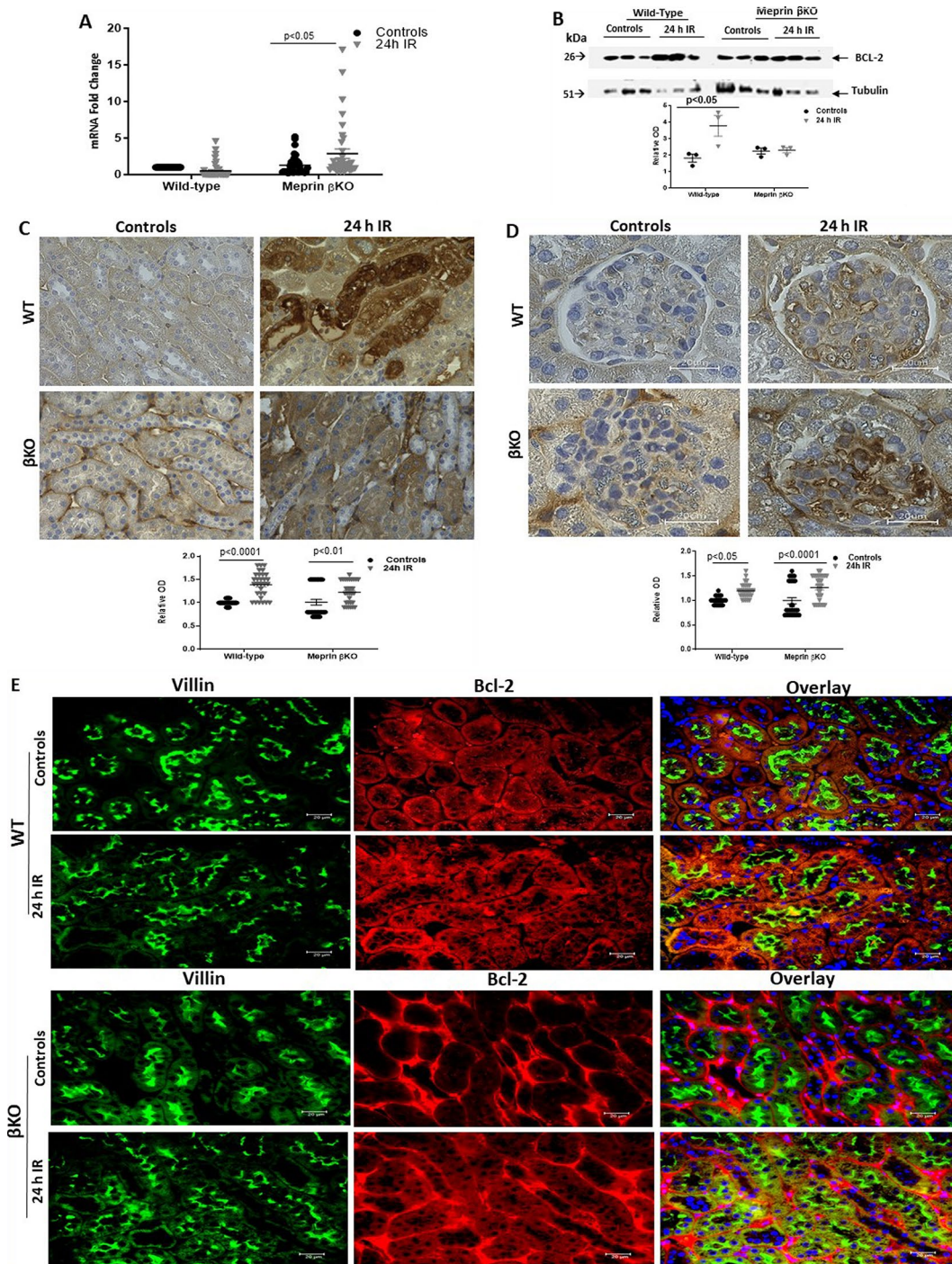


Fig. 3 Bcl-2 expression in kidney tissue from WT and meprin β KO mice at 0 h and 24 h post-IR. The real-time PCR data showed that mRNA expression levels of Bcl-2 significantly increased in β KO mice only at 24 h post-IR (A). Real-time-PCR analysis showed significant increases in Bcl-2 mRNA levels in both genotypes at 24 h post-IR. Bcl-2 mRNA levels are expressed as fold change (FC) relative to the WT control and normalized to GAPDH mRNA and each value represents the mean \pm SEM of triplicate combinations from 4 mice per group. Western blot analysis showed a significant increase of the Bcl-2 protein level in WT at 24 h post-IR but not in β KO mice (B). The protein bands of Bcl-2 detected at 26 KDa represent samples from individual kidneys ($n = 3$). The relative optic densities (ODs) were calculated by normalizing the ODs of Bcl-2 to the ODs for β -tubulin in the same sample. The full-length images of western blot are presented in supplementary figure (S3). Immunostaining of Bcl-2 showed significant increase in select tubules of both genotypes (C) and renal corpuscles (D). OD data were quantified ($n = 3$) using Image J analysis Software (ImageJ/Fiji 1.46) and analyzed for 10 non-overlapping fields from tubular and renal corpuscle sections. Images at 60 \times magnification and the scale bar representing 20 μ m. Representative immunofluorescence staining for Bcl-2 (red) in WT and meprin β KO mice kidney tubules showed that levels of Bcl-2 increased in both proximal and distal tubules for WT kidneys (E). Villin (green) was used as a proximal tubule marker in both genotypes because of antibody incompatibility. DAPI was used to stain the nuclei (blue). Images at 60 \times magnification and the scale bar representing 20 μ m. Data is expressed as mean \pm SEM with P values as indicated, $P \leq 0.05$ are considered statistically significant

increase in Bcl-2 expression in both WT and β KO kidney tissues suggests a partial association to meprin β expression. This leads us to conclude that meprin β has a modest impact on Bcl-2 anti-apoptotic effect; therefore, other mediators could be involved.

We also evaluated whether meprin β expression impacts the levels of NF κ B, a well-known pro-survival factor and one of the downstream targets of the OPN-signaling pathway. The mRNA levels of NF κ B increased significantly ($P \leq 0.0001$) in the kidneys of meprin β deficient mice at 24 h post-IR but no change was observed in WT kidneys (Fig. 4A). However, western blot analysis showed no significant change in NF κ B protein levels in either genotype (Fig. 4B), an outcome that could be attributed to the low sensitivity of this method. Immunohistochemical analysis on the other hand showed a significant increase in protein levels for NF κ B ($P \leq 0.0001$) in select tubules of WT but not β KO kidneys subjected to IR when compared to control counterparts (Fig. 4C). Staining intensity for NF κ B in renal corpuscle tissue increased significantly only in WT kidneys ($P \leq 0.01$) at 24 h post-IR (Fig. 4D). We used immunofluorescence counterstaining with proximal tubule markers to determine whether the increase in NF κ B occurs in proximal tubules (which express meprins) or distal tubules (which lack meprins). Our data showed increases in levels of NF κ B in proximal tubules of WT kidneys (Fig. 4E), suggesting that this increase correlates to meprin β expression. Meprin β could thus promote the inflammatory response in kidney injury via OPN- NF κ B signaling.

Discussion

Expression levels and localizations of meprin metalloproteases has been shown to be associated with IR-induced kidney injury [2–4, 27]. Meprins are redistributed from the BBM to the cytoplasm and basolateral compartments of proximal tubule epithelial cells in IR-induced kidney injury [2], allowing the enzymes to interact with proteins present in these cell compartments. Meprin B has been shown to proteolytically process osteopontin (OPN) [7, 31] a promising candidate that has demonstrated significance as a potential biomarker in several forms of kidney disease [8, 9, 32–38]. OPN is a highly phosphorylated multifunctional protein that plays an important role in kidney diseases such as IR-induced acute renal injury, interstitial inflammation, and fibrosis [9]. Several studies demonstrated that inhibiting OPN expression or activity can alleviate kidney injury and enhance overall kidney function through its multifunctional roles (e.g. enhances macrophage and T cells infiltration and cytokine synthesis) [39, 40]. Although OPN is recognized for promoting inflammation and cell proliferation, it has also been shown to attenuate apoptosis [41, 42], a process regulated by key apoptotic proteins, namely Bcl-2, Bax, and

Caspase-3. In addition, OPN promotes activation of NF κ B (NF κ B), a key protein that plays a vital role in regulating apoptosis [43, 44] and promotes apoptosis especially in response to cellular stress [45–47], enhancing pro-inflammatory responses that can lead to tissue damage, particularly in ischemia/reperfusion (IR) injury [40]. By promoting the expression of NF κ B target genes, OPN can amplify inflammation and contribute to tissue damage [12, 14, 48], consequently regulating the apoptotic pathway. Upon NF κ B activation in response to cellular stress, such as oxidative stress or tissue injury commonly seen in IR conditions [45–47], OPN exhibits an anti-apoptotic function by upregulating Bcl-2, thereby helping protect cells from programmed cell death [12]. Conversely, OPN also regulates apoptosis by influencing Caspase-3 activity, a critical executioner in the apoptotic pathway [13]. Elevated OPN levels are often associated with reduced Caspase-3 activation, suggesting that OPN may inhibit apoptosis and exert an anti-apoptotic effect in IR contexts [49–51]. To our knowledge, among anti-apoptotic Bcl-2 family proteins, Bcl-2 and Bcl-xl have been most extensively studied in the kidney, however, no studies have shown the effect of meprin β -OPN interactions as pro- and anti-apoptotic modulators of Caspase-3 and Bcl-2 in IR-induced AKI. Considering the contrasting roles of Bcl-2 and Caspase-3 in apoptosis regulation, we investigated how OPN mediates the balance between cell survival and death in the context of NF κ B activation and the proteolytic processing of OPN by meprin β in response to IR-induced stress. Data from the present study shows that meprin β can regulate the expression of OPN and influence the downstream mediators that regulate pro- and anti-apoptotic genes in IR-induced kidney injury. Our data corroborates a previous study that reported increased OPN staining in distal kidney tubules at 24 h after reperfusion [52]. This study by Persy et al. [52] further showed that proximal tubules exhibited a delayed rise of OPN expression, with a maximum after five days of reperfusion. In the current study, we demonstrate increased levels of OPN in the lumen of select proximal tubules of WT but not meprin β KO kidneys, suggesting meprin-associated release of OPN into the filtrate and ultimately into urine in IR-induced kidney injury. Release of OPN into urine was reported in previous studies of chronic kidney disease and nephritis [28–30]. Other study demonstrated that the concentration of cleaved forms of OPN was higher in urine of lupus nephritis (LN) patients than in healthy controls [29]. We explored further to determine how proteolytic processing of OPN by meprin β could impact downstream mediators of OPN signaling that regulate apoptosis and cell survival in IR-induced kidney injury. Cell apoptosis is under the influence of several gene products [48] Bcl-2, Bax, and Caspase-3 are the most important regulatory

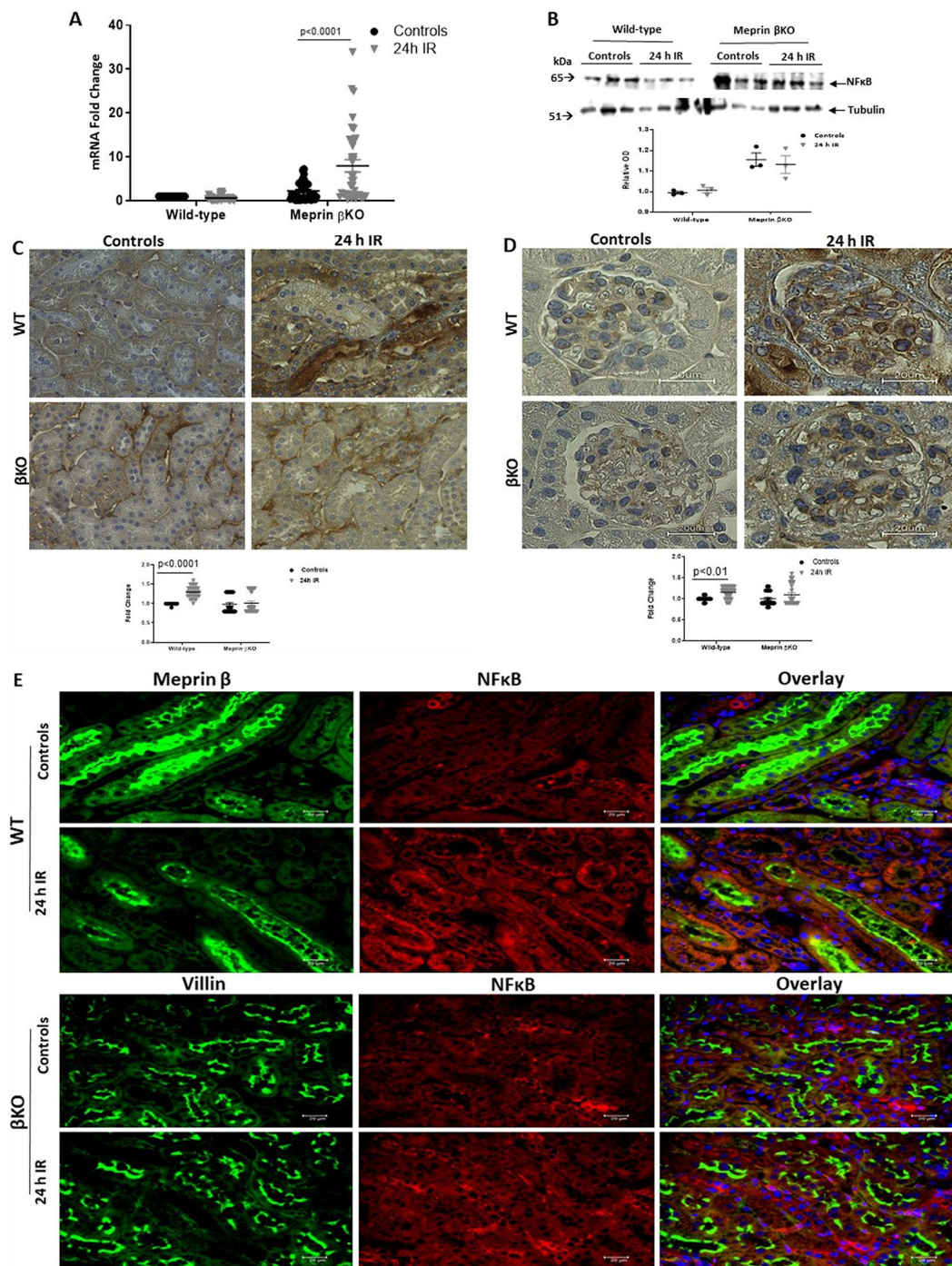


Fig. 4 NFκB expression in kidney tissue from WT and meprin βKO mice at 0 h and 24 h post-IR. The real-time PCR data showed that mRNA expression levels of NFκB increased significantly in the βKO at 24 h post-IR but not in WT kidneys (A). NFκB mRNA levels are expressed as fold change (FC) relative to the WT control and normalized to GAPDH mRNA and each value represents the mean ± SEM of triplicate combinations from 4 mice per group. Western blot analysis detected NFκB bands at 65 kDa (B). The protein bands represent samples from individual kidneys (n = 3). The relative optic densities (ODs) were calculated by normalizing the ODs of NFκB to the ODs for β-tubulin in the same sample. The full-length images of western blot are presented in supplementary figure (S4). Immunostaining of NFκB showed a significant increase in protein levels for NFκB in select tubules of WT but not βKO (C) and staining intensity for NFκB increased significantly only in WT kidneys renal corpuscles of both genotypes (D). OD data were quantified (n = 3) using Image J analysis Software (ImageJ/Fiji 1.46) and analyzed for 10 non-overlapping fields from tubular and renal corpuscle sections. Images at 60× magnification and the scale bar representing 20 μm. Immunofluorescence counterstaining of NFκB (red) with either meprin β (green) in WT or villin (PT marker, green) in in meprin β-deficient mice showed increases in levels of NFκB in proximal tubules of WT kidneys (E). DAPI was used to stain the nuclei (blue). Images at 60× magnification and the scale bar representing 20 μm. Data is expressed as mean ± SEM with P values as indicated, P ≤ 0.05 are considered statistically significant

proteins in cell apoptosis [41, 42]. Silencing of OPN by small interfering RNA decreased the Bcl-2 and increased Bax and Caspase-3 levels, in human renal carcinoma Caki-1 cells [13]. OPN-treated T cells also had increased expression of Bcl-2 and decreased expression of Bax suggesting that OPN is anti-apoptotic [43]. Because we were interested in Caspase-3 as a pro-apoptotic biomarker, we didn't include Bax in this study as it's been shown to promote cell death in response to different cellular stresses by inducing necrotic cell death in certain cases even when Caspase activation is inhibited [53]. Furthermore, Bcl-2 prevents apoptosis by inhibiting Bax [41, 54, 55] and increasing cell numbers by preventing death rather than division rate [56], along with our findings, prompting an investigation into meprin β 's role in proliferation via PCNA in IR injury [57, 58]. The data indicates a significant decrease in mRNA expression of Caspase-3, in WT tissues. In contrast, immunostaining showed that the increased Caspase-3, Bcl-2 and NF κ B protein staining occurred in select tubules in the WT kidneys. It has been documented that the level of mRNA doesn't necessarily reflect the abundance of the encoded protein [59]. In the cellular stress environment induced by IR, lower mRNA expression level compared to the protein expression level may occur due to the fact that proteins are more stable than mRNAs with an average half-life of 46 h compared to a few hours, respectively [60], post-transcriptional regulation and measurement noise [61]. Changes in post-transcriptional processes may lead to stronger deviations from an ideal correlation between mRNA and protein expression under highly dynamic phases and/or stressful conditions such IR [62]. This could also be due to "translation on demand", a mechanism that induces the translation of pre-existing transcripts, to ensure that proteins are rapidly available in response to signals without having to constitutively synthesize them [41]. Similar patterns have been shown by other studies. For example, Tian et al. reported that c-kit ligand protein had a 5-fold higher level in the mice erythroid-myeloid-lymphoid cells, but no change in mRNA levels [63]. Furthermore, Bcl-2 mRNA expression was decreased in nephrotoxic nephritis kidneys but the protein increased in some kidney tubules [64]. Another study using different models of kidney injury reported lower expression levels of Bcl-2. A high level expression of Bax and low level expression of Bcl-2 were observed in cisplatin-induced AKI on mice [65]. Also, a decrease in expression levels of Bcl-2 was observed in ESRD patients [66–68]. Thus, the difference in mRNA and protein expression should be further studied to determine which factor contributes to this inverse correlation. Our data showed that while Bcl-2 protein levels increased in both WT and meprin β knockout mice, Caspase-3 increased only in WT kidneys. This suggests that meprin β

enhances kidney injury in part by regulating the apoptotic effect of Caspase-3. The elevation in Caspase-3 and Bcl-2 protein levels in kidney tubules may indicate that the two opposing mechanisms determine the fate of the cells as previously reported [64]. Moreover, several studies suggested a feedback loop between Bcl-2 and Caspase-3. For example, Caspase-3 is known to act downstream of Bax/Bcl-2 and play a key role in execution of apoptosis [69]. Another study suggested that Bcl-2 also acts as a downstream death substrate of Caspases and that Caspases may be able to inhibit the anti-apoptotic effect of Bcl-2 [70]. Our data is aligned with findings from a previous study that demonstrated a decrease in total Bcl-2 mRNA and protein in nephrotoxic nephritis kidneys and a local increase of Bcl-2 proteins in some atrophic tubules. The same study indicated an increase in Bax transcription, translation and distribution, and the ratio of Bax/Bcl-2 increased and correlated with Caspase-3 activity in kidney [64]. The expression levels of Bcl-2 remained in proximal tubules but increased in distal tubules within 24 h of reperfusion using bilateral renal artery occlusion and it depends on the severity of injury [71]. Our recent study indicated that cell apoptosis in IR tissues might be controlled by the balance of pro-apoptotic and anti-apoptotic factors as meprin β showed high expression levels of both Caspase-3 and Bcl-2 proteins at 24 h post-IR [6]. NF κ B activation has been shown to promote the inflammatory response in kidney injury [72], enhance cell proliferation and regulate cell survival [73] and apoptosis [43, 44]. As a cell survival and anti-apoptotic molecule, NF κ B activation has been shown to be up regulated by OPN in different diseases. For example, overexpression of OPN in the kidney correlated with activation of NF κ B, increasing the expression of pro-inflammatory cytokines [40]. In synovial T cells, NF κ B was activated after treatment with OPN [43]. In addition, OPN silencing in hepatocellular carcinoma (HCC) resulted in suppression of Bcl-2 expression and NF κ B inactivation [74]. In this study we examined the effect of meprin β expression on OPN-upregulating NF κ B in IR-induced AKI. The data showed increased expression levels of NF κ B in WT proximal kidney tubules after IR, which may correlate to OPN high levels. These observations support previous studies which indicate activation of NF κ B in OPN-treated T cells [43]. In another study of OPN-upregulation of NF κ B, it was shown that OPN stimulates the transcriptional activity of NF κ B in breast cancer cells. Moreover, inhibition of NF κ B-DNA binding activity was shown to be enhanced in human gastric cancer cells by OPN siRNA [75]. Therefore, the increased level of NF κ B in proximal kidney tubules may correlate to increase OPN level and meprin β expression. Meprin β modulates the pathogenesis of inflammatory disorders through processing of several cytokines (e.g. IL-1 β , IL-6,

IL-18) [76–78]. For example, meprin β proteolytically processes IL-18 and produces active IL-18, which is known to activate the transcription factor, NF κ B [76]. Another active cytokine that is produced by both meprin β and α , is IL-1 β , which contributes to activation of NF κ B and MAPK signaling [79]. Though earlier studies have reported an anti-apoptotic activity of NF κ B [80, 81], to our knowledge no available studies implicated meprin interaction with OPN in NF κ B anti-apoptotic activity in IR-induced kidney injury. The current study examined whether meprin β expression affects the levels of three modulators of apoptosis associated with the OPN-signaling pathway, namely, Caspase-3, Bcl-2 and NF κ B and provides new insights on meprin β regulation of the pathophysiology of IR-induced acute kidney injury. An interesting observation in the present study is the increased level of OPN in meprin expressing tubules as well as in the lumen of proximal tubules of WT but not meprin β KO kidneys, suggesting enhanced release into filtrate and ultimately into urine. This leads us to conclude that proteolytic processing of OPN by meprin β plays an important role in release of OPN into urine. Our study also shows increased level of apoptotic mediator, Caspase-3, and inflammatory molecule, NF κ B, in proximal kidney tubules which may correlate to meprin β expression and/or activity. Taken together, our data showed that OPN correlates with meprin β expression and may drive apoptosis through regulation of Caspase-3. Meprin β 's role in IR-induced kidney injury extends beyond the OPN signaling pathway, involving other mechanisms like PKA-C [24], JAK/STAT [6], AKT/ERK [56, 57] pathways. Taking into account our previous findings on the role of meprins in IR [6, 24, 58], together with the current study, we propose that the hydrolytic processing of OPN by meprin β may modulate Bcl-2 and Caspase-3 levels, potentially through NF κ B and these pathways. Our findings suggest that meprin β regulates OPN downstream mediators, with further studies needed to explore additional underlying mechanisms. Although OPN is recognized for its anti-apoptotic activity in other diseases, to our knowledge, there is no available data on its role as an anti-apoptotic protein in kidney injury, particularly in the context of meprin regulation. Understanding this interplay could provide deeper insights into the mechanisms activated by meprin β in IR-induced kidney injury, revealing potential therapeutic targets for mitigating kidney injury. This study focused on meprin β isoform mice due to its established role in exacerbating IR-induced AKI [2, 82]. While the role of meprin α has been studied previously [3], we acknowledge potential compensatory effects of meprin α in β KO mice. To address this limitation, we have developed an $\alpha\beta$ double knockout model, with ongoing studies aimed at

uncovering the interplay between meprin isoforms in kidney injury.

Conclusion

In summary, the current study demonstrates that meprin β regulates the pathophysiology of IR-induced kidney injury in part via interaction with osteopontin and modulation of downstream mediators of the OPN-signaling pathway that play a role in apoptosis.

Abbreviations

2- $\Delta\Delta$ Ct method	2-(Delta Delta C(T)) Method
AKI	Acute Kidney Injury
Bax	Bcl-2 Associated X
BBM	Brush-Border Membrane
Bcl-2	B-Cell Lymphoma/Leukemia 2
Caspase-3	Cysteine-Aspartic Acid Protease-3
cDNA	Complementary Deoxyribonucleic Acid
DAPI	4,6-Diamidino-2-Phenylindole
DTs	Distal Tubules
ELISA	Enzyme-Linked Immunosorbent Assays
ESRD	End-Stage Renal Disease
FBS	Fetal Bovine Serum
FC	Fold Change
GAPDH	Glyceraldehyde-3-Phosphate Dehydrogenase
HEPES	4-(2-Hydroxyethyl)-1-Piperazineethanesulfonic Acid
IL-18	Interferon-Gamma Inducing Factor
IL-1 β	Interleukin-1 Beta
IL-6	Interleukin 6
IR	Ischemia/Reperfusion
LARU	Laboratory Animal Resource Unit of North Carolina
LN	Lupus Nephritis
Meprin A	Meprin A is a Homooligomer of α Subunits (α - α) or a Heterooligomer of α and β Subunits (α - β)
Meprin B	Meprin B is a Homooligomer of β Subunits (β - β)
mRNA	Messenger Ribonucleic Acid
NaCl	Sodium Chloride
NF κ B	Nuclear Factor Kappa-Light-Chain-Enhancer of Activated B Cells
NGAL	Neutrophil Gelatinase-Associated Lipocalin
OPN	Osteopontin
PAGE	Polyacrylamide Gels
PBS	Phosphate Buffer Saline
PCNA	Cellular Proliferation Marker
PCR	Polymerase Chain Reaction
PTs	Proximal Tubules
RIPA	Radioimmunoprecipitation Assay
RNA	Ribonucleic Acid
Scr	Serum Creatinine
SDS	Sodium Dodecyl Sulfate
TBS	Tris-Buffered Saline
TBS-T	Tris-Buffered Saline with Tween-20
TEMED	Tetramethylethylenediamine
WT	Wild-Type
β KO	Meprin- β Knockout Mice, Deficient in Meprin B (β - β) and the Heterodimeric Form of Meprin A (α - β)

Supplementary Information

The online version contains supplementary material available at <https://doi.org/10.1186/s12882-025-03995-7>.

Supplementary Material 1

Author contributions

FA: Conception, design of the work, data acquisition, data analysis, interpretation of data, drafted the work, substantively revision. SA: Conception,

design of the work, data acquisition, data analysis, interpretation of data, drafted the work, substantively revision. A. A: Data analysis, substantively revision. C. A: Data analysis, interpretation of data, substantively revision. E.O: Funding, conception, design of the work, data analysis, interpretation of data; drafting, substantively revision. F. A; S. A; A. A; C. A; E. O; Approved the submitted version and agreed to be personally accountable for their own contributions and have ensured the accuracy and integrity of any part of the work is appropriately investigated, resolved, and the resolution documented in the literature. All authors reviewed the manuscript.

Funding

This work was supported by funding from the National Institutes of Health (NIH) Award numbers SC1GM3102049 and R35GM141537 to Elimelda Moige Onger. Faihaa Ahmed was supported by NIH grant number T32 AI007273.

Data availability

The datasets used and analyzed during the current study are available from the corresponding author upon reasonable request.

Declarations

Ethics approval and consent to participate

The work in this study was reviewed and approved by the Institutional Animal Care and Use Committee (IACUC) at North Carolina A&T State University.

Consent for publication

Not applicable.

Competing interests

The authors declare no competing interests.

Received: 2 August 2024 / Accepted: 30 January 2025

Published online: 22 February 2025

References

- Sun Q, Jin H, Bond JS. Disruption of the meprin α and β genes in mice alters homeostasis of monocytes and natural killer cells. *Exp Hematol*. 2009;37(3):346–56. <https://doi.org/10.1016/j.exphem.2008.10.016>.
- Bylander J, Li Q, Ramesh G, Zhang B, Reeves WB, Bond JS. Targeted disruption of the meprin metalloproteinase β gene protects against renal ischemia-reperfusion injury in mice. *Am J Physiology-Renal Physiol*. 2008;294(3):F480–90. <https://doi.org/10.1152/ajprenal.00214.2007>.
- Herzog C, Seth R, Shah SV, Kaushal GP. Role of meprin A in renal tubular epithelial cell injury. *Kidney Int*. 2007;71(10):1009–18. <https://doi.org/10.1038/sj.ki.5002189>.
- Niyitegeka JMV, Bastidas AC, Newman RH, Taylor SS, Onger EM. Isoform-specific interactions between meprin metalloproteases and the catalytic subunit of protein kinase A: significance in acute and chronic kidney injury. *Am J Physiology-Renal Physiol*. 2015;308(1):F56–68. <https://doi.org/10.1152/ajprenal.00167.2014>.
- Red Eagle AR, Hanson RL, Jiang W, et al. Meprin β metalloprotease gene polymorphisms associated with diabetic nephropathy in the Pima Indians. *Hum Genet*. 2005;118(1):12–22. <https://doi.org/10.1007/s00439-005-0019-7>.
- Aboussad S, Ahmed F, Abouzeid A, Onger EM. Meprin β expression modulates the interleukin-6 mediated JAK2-STAT3 signaling pathway in ischemia/reperfusion-induced kidney injury. *Physiological Rep*. 2022;10(18). <https://doi.org/10.14814/phy2.15468>.
- Bertenshaw GP, Turk BE, Hubbard SJ, et al. Marked differences between metalloproteases Meprin A and B in substrate and peptide bond specificity. *J Biol Chem*. 2001;276(16):13248–55. <https://doi.org/10.1074/jbc.M011414200>.
- Xie Y, Sakatsume M, Nishi S, Narita I, Arakawa M, Gejyo F. Expression, roles, receptors, and regulation of osteopontin in the kidney. *Kidney Int*. 2001;60(5):1645–57. <https://doi.org/10.1046/j.1523-1755.2001.00032.x>.
- Kaleta B. The role of osteopontin in kidney diseases. *Inflamm Res*. 2019;68(2):93–102. <https://doi.org/10.1007/s00011-018-1200-5>.
- Cen C, Aziz M, Yang WL, Nicastro JM, Coppa GF, Wang P. Osteopontin blockade attenuates renal injury after ischemia reperfusion by inhibiting NK Cell Infiltration. *Shock*. 2017;47(1):52–60. <https://doi.org/10.1097/SHK.0000000000000721>.
- Lund SA, Giachelli CM, Scatena M. The role of osteopontin in inflammatory processes. *J Cell Commun Signal*. 2009;3(3–4):311–22. <https://doi.org/10.1007/s12079-009-0068-0>.
- Iida T, Wagatsuma K, Hirayama D, Nakase H. Is osteopontin a friend or foe of cell apoptosis in Inflammatory Gastrointestinal and Liver diseases? *IJMS*. 2017;19(1):7. <https://doi.org/10.3390/ijms19010007>.
- Zhang A, Liu Y, Shen Y, Xu Y, Li X. Osteopontin silencing by small interfering RNA induces apoptosis and suppresses invasion in human renal carcinoma Caki-1 cells. *Med Oncol*. 2010;27(4):1179–84. <https://doi.org/10.1007/s12032-009-9356-z>.
- Yoo KH, Thornhill BA, Forbes MS, et al. Osteopontin regulates renal apoptosis and interstitial fibrosis in neonatal chronic unilateral ureteral obstruction. *Kidney Int*. 2006;70(10):1735–41. <https://doi.org/10.1038/sj.ki.5000357>.
- Cheng YT, Tu YC, Chou YH, Lai CF. Protocol for renal ischemia-reperfusion injury by flank incisions in mice. *STAR Protocols*. 2022;3(4):101678. <https://doi.org/10.1016/j.xpro.2022.101678>.
- Scarfe L, Menshikh A, Newton E, et al. Long-term outcomes in mouse models of ischemia-reperfusion-induced acute kidney injury. *Am J Physiology-Renal Physiol*. 2019;317(4):F1068–80. <https://doi.org/10.1152/ajprenal.00305.2019>.
- Kanchi M, Manjunath R, Massen J, Vincent L, Belani K. Neutrophil gelatinase-associated lipocalin as a biomarker for predicting acute kidney injury during off-pump coronary artery bypass grafting. *Ann Card Anaesth*. 2017;20(3):297. https://doi.org/10.4103/aca.ACA_48_17.
- Pejović B, Erić-Marinković J, Pejović M, Kotur-Stevuljević J, Peco-Antić A. Detection of acute kidney injury in premature asphyxiated neonates by serum neutrophil gelatinase-associated lipocalin (sNGAL)— sensitivity and specificity of a potential new biomarker. *Biochem Med Published Online*. 2015;450–9. <https://doi.org/10.11613/BM.2015.046>.
- Nakhjavan-Shahraki B, Youseffard M, Ataei N, et al. Accuracy of cystatin C in prediction of acute kidney injury in children; serum or urine levels: which one works better? A systematic review and meta-analysis. *BMC Nephrol*. 2017;18(1):120. <https://doi.org/10.1186/s12882-017-0539-0>.
- Javan AO, Salamzadeh J, Shokouhi S, Sahraei Z. Evaluation of renal toxicity of Colistin Therapy with Neutrophil Gelatinase-associated Lipocalin: A Biomarker of Renal Tubular Damage. *Iran J Kidney Dis*. 2017;11(6):447–455.
- He Z, Tang H, You X, et al. BAPTA-AM nanoparticle for the curing of Acute kidney injury Induced by Ischemia/Reperfusion. *J Biomed Nanotechnol*. 2018;14(5):868–83. <https://doi.org/10.1166/jbn.2018.2532>.
- Chai X, Huang HB, Feng G, et al. Baseline serum cystatin C is a potential predictor for acute kidney injury in patients with Acute Pancreatitis. *Dis Markers*. 2018;2018:1–7. <https://doi.org/10.1155/2018/8431219>.
- Kamel NM, Abd El Fattah MA, El-Abhar HS, Abdallah DM. Novel repair mechanisms in a renal ischaemia/reperfusion model: subsequent saxagliptin treatment modulates the pro-angiogenic GLP-1/cAMP/VEGF, ANP/eNOS/NO, SDF-1 α /CXCR4, and Kim-1/STAT3/HIF-1 α /VEGF/eNOS pathways. *Eur J Pharmacol*. 2019;861:172620. <https://doi.org/10.1016/j.ejphar.2019.172620>.
- Ahmed F, Mwiza JM, Fernandez M, Yahaya I, Aboussad S, Onger EM. Meprin- β activity modulates the β -catalytic subunit of protein kinase A in ischemia-reperfusion-induced acute kidney injury. *Am J Physiology-Renal Physiol*. 2020;318(5):F1147–59. <https://doi.org/10.1152/ajprenal.00571.2019>.
- Chapman J, Miles PD, Ofrecio JM et al. Osteopontin Is Required for the Early Onset of High Fat Diet-Induced Insulin Resistance in Mice. *Polidori C, ed. PLoS ONE*. 2010;5(11):e13959. <https://doi.org/10.1371/journal.pone.0013959>.
- Schmittgen TD, Livak KJ. Analyzing real-time PCR data by the comparative CT method. *Nat Protoc*. 2008;3(6):1101–8. <https://doi.org/10.1038/nprot.2008.73>.
- Onger EM, Anyanwu O, Reeves WB, Bond JS. Villin and actin in the mouse kidney brush-border membrane bind to and are degraded by meprins, an interaction that contributes to injury in ischemia-reperfusion. *Am J Physiology-Renal Physiol*. 2011;301(4):F871–82. <https://doi.org/10.1152/ajprenal.00703.2010>.
- Feldreich T, Carlsson AC, Helmersson-Karlqvist J, et al. Urinary osteopontin predicts incident chronic kidney disease, while plasma Osteopontin predicts Cardiovascular Death in Elderly men. *Cardiorenal Med*. 2017;7(3):245–54. <https://doi.org/10.1159/000476001>.
- Kitagori K, Yoshifuji H, Oku T et al. M Kuwana ed. 2016 Cleaved form of Osteopontin in urine as a clinical marker of Lupus Nephritis. *PLoS ONE* 11 12 e0167141 <https://doi.org/10.1371/journal.pone.0167141>.
- Lorenzen J, Shah R, Biser A, et al. The role of Osteopontin in the development of Albuminuria. *J Am Soc Nephrol*. 2008;19(5):884–90. <https://doi.org/10.1681/ASN.2007040486>.
- Villa JP, Bertenshaw GP, Bylander JE, Bond JS. Meprin proteolytic complexes at the cell surface and in extracellular spaces. *Saklatvala J, Nagase H, Salvesen G,*

- eds. *Biochemical Society Symposia*. 2003;70:53–63. <https://doi.org/10.1042/bss0700053>
32. Nicholas SB, Liu J, Kim J, et al. Critical role for osteopontin in diabetic nephropathy. *Kidney Int*. 2010;77(7):588–600. <https://doi.org/10.1038/ki.2009.518>.
 33. Moszczuk B, Krata N, Rudnicki W, et al. Osteopontin—A potential biomarker for IgA Nephropathy: machine learning application. *Biomedicines*. 2022;10(4):734. <https://doi.org/10.3390/biomedicines10040734>.
 34. Wirestam L, Enocsson H, Skogh T, et al. Osteopontin and Disease Activity in patients with recent-onset systemic lupus erythematosus: results from the SLICC Inception Cohort. *J Rheumatol*. 2019;46(5):492–500. <https://doi.org/10.3899/jrheum.180713>.
 35. Steinbrenner I, Sekula P, Kotsis F, et al. Association of osteopontin with kidney function and kidney failure in chronic kidney disease patients: the GCKD study. *Nephrol Dialysis Transplantation*. 2023;38(6):1430–8. <https://doi.org/10.1093/ndt/gfac173>.
 36. Trostel J, Truong LD, Roncal-Jimenez C, et al. Different effects of global osteopontin and macrophage osteopontin in glomerular injury. *Am J Physiology-Renal Physiol*. 2018;315(4):F759–68. <https://doi.org/10.1152/ajprenal.00458.2017>.
 37. Gordin D, Forsblom C, Panduru NM, et al. Osteopontin is a strong predictor of Incipient Diabetic Nephropathy, Cardiovascular Disease, and all-cause mortality in patients with type 1 diabetes. *Diabetes Care*. 2014;37(9):2593–600. <https://doi.org/10.2337/dc.14-0065>.
 38. Kim H, Sung J, Bae JY, Lee P, Oh YK, Kim H. Identification of osteopontin as a urinary biomarker for autosomal dominant polycystic kidney disease progression. *Kidney Res Clin Pract*. 2022;41(6):730–40. <https://doi.org/10.23876/j.krcp.21.303>.
 39. Mezzano SA, Droguett MA, Burgos ME, et al. Overexpression of chemokines, fibrogenic cytokines, and myofibroblasts in human membranous nephropathy. *Kidney Int*. 2000;57(1):147–58. <https://doi.org/10.1046/j.1523-1755.2000.0830.x>.
 40. Mezzano SA, Barria M, Droguett MA, et al. Tubular NF- κ B and AP-1 activation in human proteinuric renal disease. *Kidney Int*. 2001;60(4):1366–77. <https://doi.org/10.1046/j.1523-1755.2001.00941.x>.
 41. Liu Q, Si T, Xu X, Liang F, Wang L, Pan S. Electromagnetic radiation at 900 MHz induces sperm apoptosis through bcl-2, bax and caspase-3 signaling pathways in rats. *Reprod Health*. 2015;12(1):65. <https://doi.org/10.1186/s12978-015-0062-3>.
 42. Sun Y, Lin Y, Li H, Liu J, Sheng X, Zhang W. 2,5-Hexanedione induces human ovarian granulosa cell apoptosis through BCL-2, BAX, and CASPASE-3 signaling pathways. *Arch Toxicol*. 2012;86(2):205–15. <https://doi.org/10.1007/s00204-011-0745-7>.
 43. Fan K, Dai J, Wang H, et al. Treatment of collagen-induced arthritis with an anti-osteopontin monoclonal antibody through promotion of apoptosis of both murine and human activated T cells. *Arthritis Rheumatism*. 2008;58(7):2041–52. <https://doi.org/10.1002/art.23490>.
 44. Schmitz ML, Mattioli I, Buss H, Kracht M. NF- κ B: a multifaceted transcription factor regulated at several levels. *ChemBioChem*. 2004;5(10):1348–58. <https://doi.org/10.1002/cbic.200400144>.
 45. Perkins ND, Gilmore TD. Good cop, bad cop: the different faces of NF- κ B. *Cell Death Differ*. 2006;13(5):759–72. <https://doi.org/10.1038/sj.cdd.4401838>.
 46. Radhakrishnan SK, Kamalakaran S. Pro-apoptotic role of NF- κ B: implications for cancer therapy. *Biochimica et Biophys Acta (BBA) - Reviews Cancer*. 2006;1766(1):53–62. <https://doi.org/10.1016/j.bbcan.2006.02.001>.
 47. Strozzyk E, Pöppelmann B, Schwarz T, Kulms D. Differential effects of NF- κ B on apoptosis induced by DNA-damaging agents: the type of DNA damage determines the final outcome. *Oncogene*. 2006;25(47):6239–51. <https://doi.org/10.1038/sj.onc.1209655>.
 48. Li Y, Lin L, Wang Q. Correlation of expression levels of caspase-3 and Bcl-2 in alveolar lavage fluid in neonatal respiratory distress syndrome and prognosis. *Exp Ther Med*. Published online January 16, 2018. <https://doi.org/10.3892/etm.2018.5755>
 49. Graessmann M, Berg B, Fuchs B, Klein A, Graessmann A. Chemotherapy resistance of mouse WAP-SVT/t breast cancer cells is mediated by osteopontin, inhibiting apoptosis downstream of caspase-3. *Oncogene*. 2007;26(20):2840–50. <https://doi.org/10.1038/sj.onc.1210096>.
 50. Gu T, Ohashi R, Cui R, et al. Osteopontin is involved in the development of acquired chemo-resistance of cisplatin in small cell lung cancer. *Lung Cancer*. 2009;66(2):176–83. <https://doi.org/10.1016/j.lungcan.2009.02.004>.
 51. Huang H, Zhang X, Zhou H, et al. Expression and prognostic significance of osteopontin and caspase-3 in hepatocellular carcinoma patients after curative resection. *Cancer Sci*. 2010;101(5):1314–9. <https://doi.org/10.1111/j.1349-7006.2010.01524.x>.
 52. Persy VP, Verstrepen WA, Ysebaert DK, De Greef KE, De Broe ME. Differences in osteopontin up-regulation between proximal and distal tubules after renal ischemia/reperfusion. *Kidney Int*. 1999;56(2):601–11. <https://doi.org/10.1046/j.1523-1755.1999.00581.x>.
 53. Karch J, Molkenin JD. Regulated necrotic cell death: the Passive Aggressive side of Bax and Bak. *Circul Res*. 2015;116(11):1800–9. <https://doi.org/10.1161/CIRCRESAHA.116.305421>.
 54. Mohan S, Abdelwahab SI, Kamalidehghan B, et al. Involvement of NF- κ B and Bcl2/Bax signaling pathways in the apoptosis of MCF7 cells induced by a xanthone compound pyranocycloartobioxanthone A. *Phytomedicine*. 2012;19(11):1007–15. <https://doi.org/10.1016/j.phymed.2012.05.012>.
 55. Hector S, Prehn JHM. Apoptosis signaling proteins as prognostic biomarkers in colorectal cancer: a review. *Biochimica et Biophys Acta (BBA) - Reviews Cancer*. 2009;1795(2):117–29. <https://doi.org/10.1016/j.bbcan.2008.12.002>.
 56. Hardwick JM, Soane L. Multiple functions of BCL-2 family proteins. *Cold Spring Harb Perspect Biol*. 2013;5(2):a008722–008722. <https://doi.org/10.1101/cshperspect.a008722>.
 57. Aboussaad S, Ahmed F, Abouzeid A, Ongeri E. Meprin β Modulates Cellular Proliferation Through The IL-6 Signaling Pathway In IRInduced Kidney Injury. *The FASEB Journal*. 2022;36(S1):fasebj.2022.36.S1.R5824. <https://doi.org/10.1096/fasebj.2022.36.S1.R5824>
 58. Aboussaad S, Ahmed F, Abouzeid A, Ongeri EM. Meprin β activity modulates Cellular Proliferation via Trans-Signaling IL-6-Mediated AKT/ERK Pathway in Ischemia/Reperfusion (IR)-Induced kidney Injury: FR-PO168. *J Am Soc Nephrol*. 2023;34(11S):451–451. <https://doi.org/10.1681/ASN.20233411S1451c>.
 59. Bishop DJ, Hawley JA. Reassessing the relationship between mRNA levels and protein abundance in exercised skeletal muscles. *Nat Rev Mol Cell Biol*. 2022;23(12):773–4. <https://doi.org/10.1038/s41580-022-00541-3>.
 60. Schwanhäusser B, Busse D, Li N, et al. Global quantification of mammalian gene expression control. *Nature*. 2011;473(7347):337–42. <https://doi.org/10.1038/nature10098>.
 61. Vogel C, Marcotte EM. Insights into the regulation of protein abundance from proteomic and transcriptomic analyses. *Nat Rev Genet*. 2012;13(4):227–32. <https://doi.org/10.1038/nrg3185>.
 62. Cheng Z, Teo G, Krueger S, et al. Differential dynamics of the mammalian mRNA and protein expression response to misfolding stress. *Mol Syst Biol*. 2016;12(1):855. <https://doi.org/10.1525/msb.20156423>.
 63. Tian Q, Stepaniants SB, Mao M, et al. Integrated genomic and proteomic analyses of Gene expression in mammalian cells. *Molecular Cellular Proteomics*. 2004;3(10):960–9. <https://doi.org/10.1074/mcp.M400055-MCP200>.
 64. Yang B, Johnson TS, Thomas GL, et al. A shift in the Bax/Bcl-2 balance may activate caspase-3 and modulate apoptosis in experimental glomerulonephritis. *Kidney Int*. 2002;62(4):1301–13. <https://doi.org/10.1111/j.1523-1755.2002.kid587.x>.
 65. Hao Q, Xiao X, Zhen J, et al. Resveratrol attenuates acute kidney injury by inhibiting death receptor-mediated apoptotic pathways in a cisplatin-induced rat model. *Mol Med Rep*. 2016;14(4):3683–9. <https://doi.org/10.3892/mmr.2016.5714>.
 66. Dounousi E, Koliouisi E, Papagianni A, et al. Mononuclear leukocyte apoptosis and inflammatory markers in patients with chronic kidney disease. *Am J Nephrol*. 2012;36(6):531–6. <https://doi.org/10.1159/000345352>.
 67. Nour H, Zahran N, Elhamid SA, Zahran M, Raafat M, Saeed AE. The role of BCL-2 and BAK genes in chronic kidney disease and haemodialysis patients. *Galuska SP, ed. JGM*. 2016;1(1):8–24. <https://doi.org/10.14302/issn.2572-5424/jgm-15-815>
 68. Majewska E, Baj Z, Sulowska Z, Rysz J, Luciak M. Effects of Uraemia and haemodialysis on neutrophil apoptosis and expression of apoptosis-related proteins. *Nephrol Dialysis Transplantation*. 2003;18(12):2582–8. <https://doi.org/10.1093/ndt/gfg441>.
 69. Rudel T. Caspase inhibitors in prevention of apoptosis. *Herz*. 1999;24(3):236–41. <https://doi.org/10.1007/BF03044967>.
 70. Cheng EHY, Kirsch DG, Clem RJ, et al. Conversion of Bcl-2 to a bax-like death effector by Caspases. *Science*. 1997;278(5345):1966–8. <https://doi.org/10.1126/science.278.5345.1966>.
 71. Gobé G, Zhang XJ, Willgoss DA, Schoch E, Hogg NA, Endre ZH. Relationship between expression of Bcl-2 genes and growth factors in ischemic Acute Renal failure in the rat. *J Am Soc Nephrol*. 2000;11(3):454–67. <https://doi.org/10.1681/ASN.V113454>.

72. Taganov KD, Boldin MP, Chang KJ, Baltimore D. NF- κ B-dependent induction of microRNA miR-146, an inhibitor targeted to signaling proteins of innate immune responses. *Proc Natl Acad Sci USA*. 2006;103(33):12481–6. <https://doi.org/10.1073/pnas.0605298103>.
73. Martinka S, Bruggeman LA. Persistent NF- κ B activation in renal epithelial cells in a mouse model of HIV-associated nephropathy. *Am J Physiology-Renal Physiol*. 2006;290(3):F657–65. <https://doi.org/10.1152/ajprenal.00208.2005>.
74. Zhao J, Dong L, Lu B, et al. Down-regulation of Osteopontin suppresses growth and Metastasis of Hepatocellular Carcinoma Via Induction of Apoptosis. *Gastroenterology*. 2008;135(3):956–68. <https://doi.org/10.1053/j.gastro.2008.05.025>.
75. Gong M, Lu Z, Fang G, Bi J, Xue X. A small interfering RNA targeting osteopontin as gastric cancer therapeutics. *Cancer Lett*. 2008;272(1):148–59. <https://doi.org/10.1016/j.canlet.2008.07.004>.
76. Banerjee S, Bond JS. Prointerleukin-18 is activated by Meprin β in Vitro and in Vivo in intestinal inflammation. *J Biol Chem*. 2008;283(46):31371–7. <https://doi.org/10.1074/jbc.M802814200>.
77. Herzog C, Haun RS, Kaushal V, Mayeux PR, Shah SV, Kaushal GP. Meprin A and meprin α generate biologically functional IL-1 β from pro-IL-1 β . *Biochem Biophys Res Commun*. 2009;379(4):904–8. <https://doi.org/10.1016/j.bbrc.2008.12.161>.
78. Keiffer TR, Bond JS. Meprin metalloproteases inactivate interleukin 6. *J Biol Chem*. 2014;289(11):7580–8. <https://doi.org/10.1074/jbc.M113.546309>.
79. Herzog C, Haun RS, Kaushal GP. Role of meprin metalloproteinases in cytokine processing and inflammation. *Cytokine*. 2019;114:18–25. <https://doi.org/10.1016/j.cyto.2018.11.032>.
80. Luo JL, IKK/NF- κ B signaling: balancing life and death - a new approach to cancer therapy. *J Clin Invest*. 2005;115(10):2625–32. <https://doi.org/10.1172/JCI26322>.
81. Sugiyama H, Savill JS, Kitamura M, Zhao L, Stylianou E. Selective sensitization to Tumor Necrosis Factor- α -induced apoptosis by blockade of NF- κ B in primary glomerular Mesangial cells. *J Biol Chem*. 1999;274(28):19532–7. <https://doi.org/10.1074/jbc.274.28.19532>.
82. Carmago S, Shah SV, Walker PD. Meprin, a brush-border enzyme, plays an important role in hypoxic/ischemic acute renal tubular injury in rats. *Kidney Int*. 2002;61(3):959–66. <https://doi.org/10.1046/j.1523-1755.2002.00209.x>.

Publisher's note

Springer Nature remains neutral with regard to jurisdictional claims in published maps and institutional affiliations.